Superconductor Science and Technology

PAPER

Critical currents of Rutherford MgB_2 cables compacted by two-axial rolling

To cite this article: L Kopera *et al* 2017 *Supercond. Sci. Technol.* **30** 015002

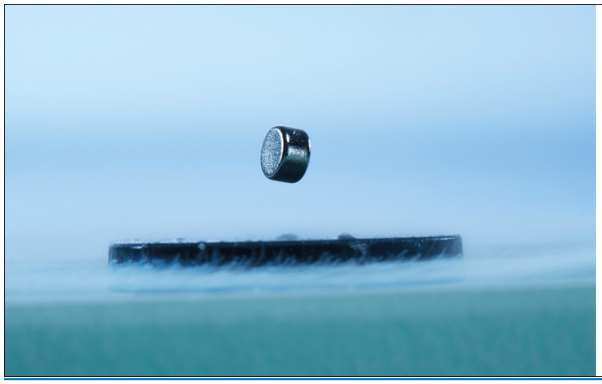

IOP Publishing Superconductor Science and Technology
Supercond. Sci. Technol. 30 (2017) 015002 (6pp) doi:10.1088/0953-2048/30/1/015002

Critical currents of Rutherford MgB_2 cables compacted by two-axial rolling

L Kopera[1], P Kováč[1], M Kulich, T Melišek[1], M Rindfleisch[2], J Yue[2] and I Hušek[1]

[1] Institute of Electrical Engineering, Slovak Academy of Sciences, Dúbravska cesta 9, 841 04 Bratislava, Slovakia
[2] HyperTech Research, Inc., Columbus, OH, USA

E-mail: Lubomir.Kopera@savba.sk

Received 14 July 2016, revised 26 September 2016
Accepted for publication 29 September 2016
Published 2 November 2016

Abstract

Two types of Rutherford cables made of two strand layers of commercial MgB_2 wires manufactured by Hyper Tech Research, Inc. have been made. Flat rectangular cables consisting of 12 single-core MgB_2/Nb/Cu10Ni, or 6-filaments MgB_2/Nb/Cu strands, both of diameter 390 mewm, were assembled using a back-twist cabling machine with transposition length of 20 mm. In order to analyze impact of the cable compaction on critical currents, cables were two-axially rolled, each by a single step reduction of 3.5%−29.7% to thickness range of 0.775−0.62 mm. It was found that by increasing the packing factor (PF) of cable above 0.79, the critical current begins to increase. It is improved nearly two times up to the PF limit 0.89. Compaction over the PF limit introduced cable degradation and decrease of critical current. Bending tests applied to cables showed that critical current degradation starts below the bending diameter 120 mm for 6-filaments Cu sheath and 70 mm for single-core Cu10Ni sheath cable. Tensile tests showed similar irreversible strain values for the both types of cables. Rutherford cables assembled of single-core strands are promising for low field (2.7−4 T) applications where low bending diameters are required.

Keywords: Rutherford cable, MgB_2, critical currents, electro-mechanical properties

(Some figures may appear in colour only in the online journal)

1. Introduction

Up to the present time several MgB_2 cables of different configurations stranded from single-core or multi-filamentary wires have been published [1–7]. It was shown that low filament density of as-drawn wires is the main limiting factor to achieve high current density of cables [2]. Since no apparent degradation during the cabling procedure of as-drawn single-core wires has been observed [2, 3], certain critical current degradation was presented for cables made of very thin filament strands [4, 5]. Holubek *et al* have shown an effective improvement of critical current of cable by rotary swaging prior to annealing [3]. Also circular cable made of Hyper Tech Research, Inc. wires demonstrated that additional mechanical deformation prior to heat treatment (by swaging, rolling or pressing) leads to a considerable enhancement of critical current in mono-filament MgB_2 cable produced by in situ technique. The engineering current density of 10^4 A cm^{-2} was measured at 4.2 K and 7 T after pressing the cable by 1.8 GPa [6].

Cables in comparison to monolithic conductors offer the following advantages: (i) easier scaling up of total current, e.g. for power cables or busbars or in low-inductance magnets, (ii) improvement of the tolerance to bending strain (smaller coils diameters made by 'react and wind' technique) and (iii) decreasing of ac losses (reduction of coupling currents). Electrical, mechanical and geometrical properties can be optimized by the total number and type of conductors and their arrangement in the cable. For example, Ballarino *et al* designed composite multi-conductor MgB_2 cable having a total current capacity of over 100 kA at 20 K [8]. The optimization may further reduce the development costs by omitting the widely accepted practice to develop a new type of conductor for the each new application. To maximize the engineering current density of winding, cables should advantageously have a rectangular cross-section. The fill

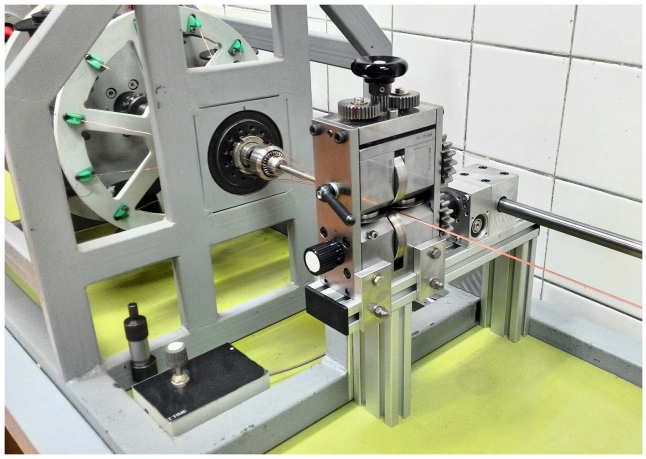

Figure 1. Cabling machine with detail of powered roller die used for compacting the cable.

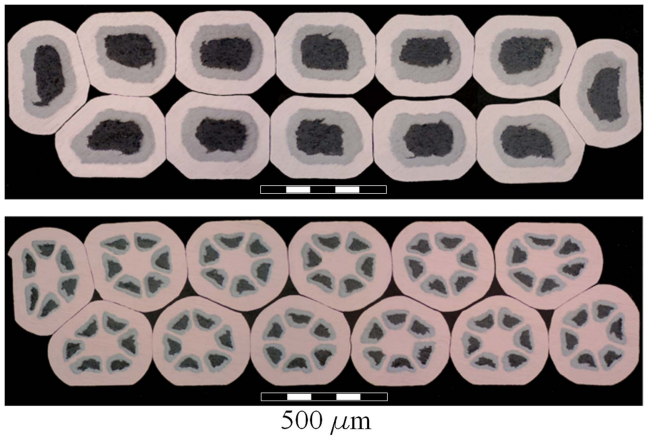

Figure 2. Magnified view of cross-section of H1R and H6R Rutherford cables transposed of single-core (up) and 6-filament wires.

factor of the winding made of rectangular cable can be theoretically increased by factor of 1.27 in comparison to a winding made of circular cable. Compared with a single rectangular conductor, the Rutherford cable is more flexible and easier to bend over a small radius of sharply curved windings or small-aperture magnets. Short transposition length and inter-strands resistance enable reduce AC losses by depressing of coupling currents [9], which are the main source of the heat generated in the winding. Analogous like the circular cables, also Rutherford type MgB_2 cables can be optimized to reach electromagnetic criteria of the final application. But the optimization may depend also on construction criteria—like the heat transfer, stability, Lorenz forces and positional accuracy of the turns in the winding, which may result in an additional compaction or adjustment of the cable shape or dimensions.

In our previous work [7] we presented manufacturing technique of Rutherford MgB_2 cable made from thin 0.3 mm single-core strands formed by 'passive' and less adaptable forming roller. Present paper shows how the additional compaction of Rutherford cable by driven two-axial forming roller can increase the density of MgB_2 strands (single- and multi-cores) by well controlled manner and consequently to optimize the current density effectively.

2. Experimental

Mono- and multi-filamentary conductors with Nb barrier and Cu10Ni or Cu outer sheath were manufactured by Hyper Tech Research [10]. Un-doped conductors were filled by mixture of fine (10–100 nm) mostly amorphous pure boron powder from Specialty Materials Inc. (SMI) and elemental (99% purity) magnesium of maximum 20–25 μm particle size. For carbon doping we used 2 mol% C doped fine B powder (10–100 nm particle size) from SMI produced by the plasma assisted reaction of BCl_3 with H_2 and *in situ* C doped by adding CH_4 to the gas mixtures [11]. Volume fraction of Mg+B mixture in strands was determined from metallographic specimens of the final as-drawn wires using an optical imaging application. Composition of both types of wires named H1W and H6W as well as their Mg+B volume fractions are specified in table 1. Both cold drawn conductors of the final diameter of 390 μm and length ~150 m were divided into 12 spools of back-twist cabling machine. The cabling system consists of stranding machine with 12 back-twist supply spools, powered forming roller (see the detail in figure 1), caterpillar, and take-up reeling machine [7]. Back-twist of spools is important to obtain a stable structure of the cable without residual torque. The wires were cabled and twisted at the same time in the opposite direction with respect to the cable axis at the ratio of one twist for one turn of the cabler (planetary motion of spools around the cable axis). All modules of the cabling system are synchronized to allow continuous control of the cabling speed versus transposition length. Initially, the 12 conductors are helically stranded around mandrel fixed in central axis of the stranding rotation. The leading part of the mandrel has circular cross-section which gradually transitions into a flat trailing end, and allows the strands to be re-arranged into flat profile. The shaped strands enter from the trailing end of the mandrel into powered roller head where compacting and final rectangular shaping of the Rutherford cable is performed. The powered roller minimizes the tensile load applied to the cable which has tendency to collapse under the tension needed to form it. Finally, two types of 12-strands cables named H1R (cabled from H1W wires) and H6R (cabled from H6W wires) with transposition length 20 mm were prepared, see tables 2 and 3.

Forming the wire strands in the roller die is a critical operation influencing the final properties of cable. Generally, 12-strand cables with not-deformed wires will occupy a rectangular area of width $6.73d$ (d = strand diameter) and minimum thickness $2d$. The packing factor (PF) of un-compacted flat cable is 0.7—it is less as the fill factor of a solenoidal type coil with square winding pattern made of a single circular wire (0.785). Increasing the compaction of MgB_2 cable increases the PF (by elimination of void area), powder density of the Mg+B filaments and contact surface among strands, which improve I_c and stability of the cable. It could be assumed that the cable compaction will have some limits

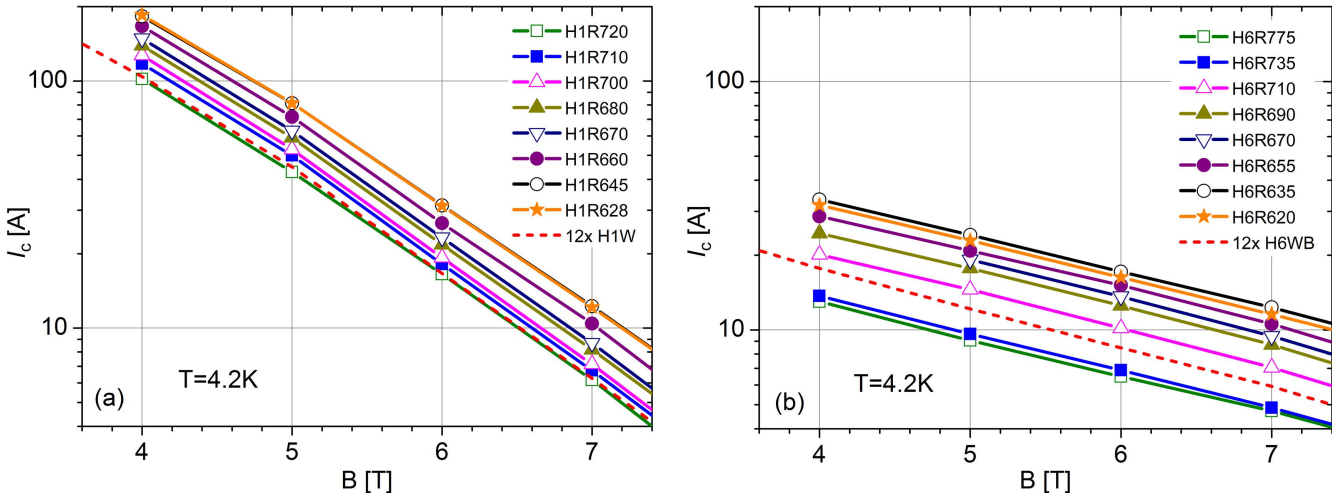

Figure 3. Critical currents of H1R (a) and H6R (b) Rutherford cables.

Table 1. MgB_2 strands used for cabling.

Strand	Filament	Barrier	Sheath	Powder material	Diameter (mm)	Mg+B (%)
H6W	6	Nb	Cu	C-doped	0.39	12.7
H1W	1	Nb	Cu10Ni	un-doped	0.39	19.8

Table 2. Thickness and packing factor of 12-strands H1R cables.

	H1R720	H1R710	H1R700	H1R680	H1R670	H1R660	H1R645	H1R628
Thickness	0.72	0.71	0.7	0.68	0.67	0.66	0.645	0.628
PF	0.781	0.792	0.803	0.827	0.839	0.852	0.872	0.895

Table 3. Thickness and packing factor of 12-strands H6R cables.

	H6R775	H6R735	H6R710	H6R690	H6R670	H6R655	H6R635	H6R620
Thickness	0.775	0.735	0.71	0.69	0.67	0.655	0.635	0.62
PF	0.725	0.765	0.792	0.815	0.839	0.858	0.885	0.907

after which I_c degradation has to occur. In order to determine the upper limit of compaction, a set of cable samples were transversally compacted by two axial rolling using single reduction step to range of thicknesses from 0.78 up to 0.62 mm. Constant width of 2.55 mm was retained for all cables.

Figure 2 shows cross-sections of H1R and H6R Rutherford cables compacted to thickness 0.67 mm. Clearly visible is the amount of compaction applied by two axial rolling by the flattened surface of strands which were initially cylindrical.

The cabling process and additional compaction of the cable samples was made on unreacted wires, prior to MgB_2 phase formation. Thereafter heat treatment for I_c-optimization was performed. The highest values for H1R cable samples and H1W strands were attained at 650 °C for 20 min in Ar atmosphere. Samples H6R and H6W were heat treated at 650 °C for 40 min in Ar atmosphere to attain the highest I_c. Due to correct I_c measurements the short cable samples (70–100 mm long pieces) were solder plated in Pb40Sn60 solder bath. It enabled correct measurement of $I-V$ curves, estimate I_c by the criterion of 1 μV cm^{-1} and improve thermal stability of samples during measurement (go to elevated currents and voltages without quenching). The solder layer was partially wiped away of the cable surface and only gaps and voids remain filled by the solder. Critical current of individual straight cables and wires as well as cables bent to diameters 20–120 mm have been measured at 4.2 K in the external magnetic field range of 1.5–8 T. Stress−strain $\sigma(\varepsilon)$ and $I_c(\varepsilon)$ characteristics of H1R and H6R cables were measured at 4.2 K in external magnetic field 6 T. The stress−strain characteristics of heat treated H1W and H6W wires were measured at room temperature only.

3. Results and discussion

Results presenting $I_c(B)$ characteristics of H1R and H6R cables are summarized in figure 3. Apparently, trend of the I_c

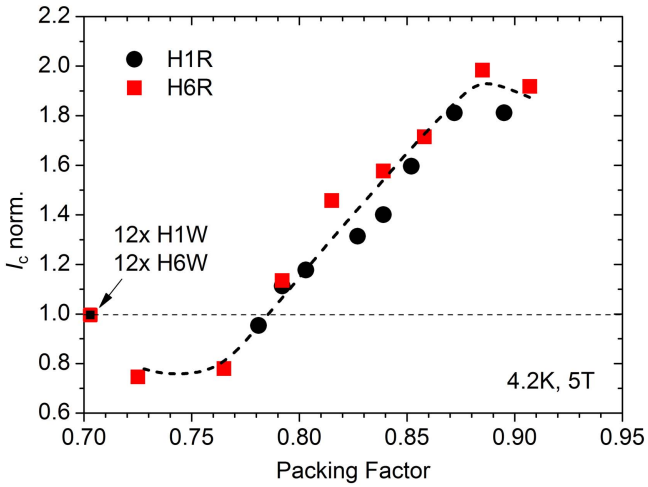

Figure 4. I_c of H1R and H6R cables normalized to 12 times I_c of as-drawn wires.

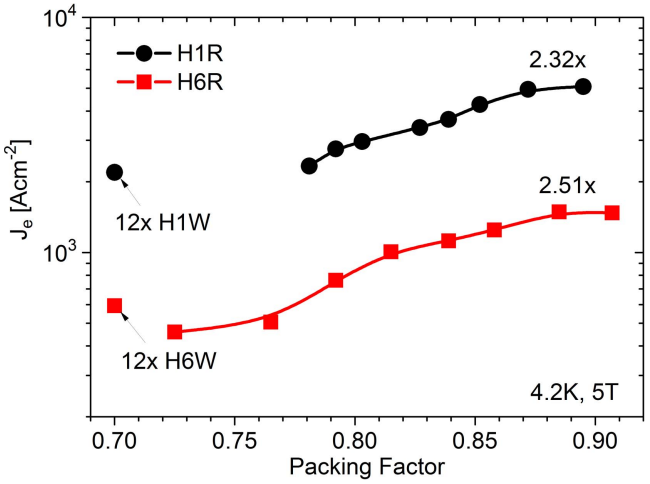

Figure 6. Engineering current density of cables H1R and H6R measured at 5 T in LHe.

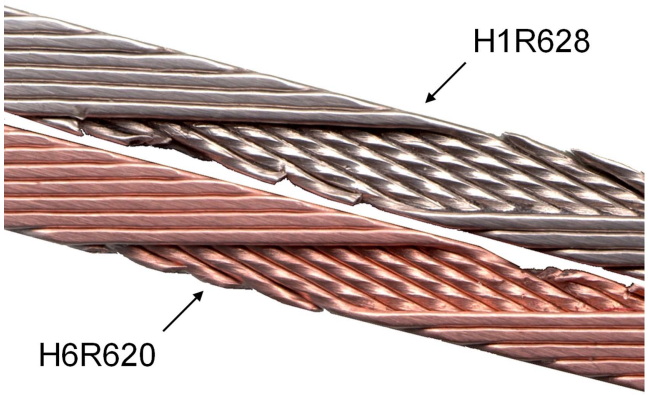

Figure 5. Imprints on crossing zones between strands of highly compacted H1R and H6R cables.

increase with decreasing the cable thickness is common for both types of cables. Such trend has been expected since the filaments density in MgB_2 strands increases with the compaction rate.

By comparing the critical currents of the H1W or H6W reference wire, one can see that only cables compacted to thickness less than 0.71 mm (PF $>$ 0.79) exhibit higher I_c than 12-times I_c of the reference wire. This can be attributed mostly to locally reduced core density of strands which are forced to bend over a very small radius on the cable edges and, to a lesser degree, to the tension load applied to strands during cabling. But, by increasing the degree of compaction the core density improves to reach considerable higher critical current. Nearly two times higher I_c was measured at 5 T for cables H1R645 and H6R635 compacted to thickness 0.645 mm and 0.635 mm, respectively (see figure 4). It corresponds to PF values 0.87–0.89. This I_c improvement is similar to circular MgB_2 cables subjected to additional densification of filaments [2, 3, 6].

At a higher degree of compaction (PF $>$ 0.89) I_c degradation was measured, which results from highly deformed strands on the cable edges and locally deformed zones at the crossing between wires. Figure 5 shows exposed bottom layer of strands after removing its upper layer on highly compacted H1R628 and H6R620 cables. Well visible are imprints due to pinching of the strands at the crossing zone between wires.

This implies that limit of the PF for both 12-strands MgB_2 Rutherford cables can be determined to PF $\sim$ 0.89. Figure 6 compares the engineering current densities on the PF for H1R and H6R cables. Due to densified filaments and increased PF of cables, the degree of increasing J_e is higher (2.32 and 2.51 times) than the increase of I_c (1.81 and 1.98 times).

Besides the degree of compacting, the influence of tensile load and flexural load applied perpendicular to the cable plane is very important for specifying a cable for practical applications. In order to characterize the influence of bending diameter (D) on the critical current degradation, $I_c(D)$ dependencies of H1R and H6R cables were measured and compared with two additional samples having different construction, but similar outer dimensions. The first sample was SC tape with 19 MgB_2 filaments embedded in Ni matrix (without diffusion barrier) of outer dimension 3 $\times$ 0.7 mm made by Columbus Superconductors [12]. Second one was Rutherford cable [7] of outer dimensions 2 $\times$ 0.54 mm stranded from twelve single-core MgB_2 wires with MONEL® 400 outer sheath [13] and Ti barrier. A comparison in figure 7 shows that the cable H1R645 with Cu10Ni sheath has a higher tolerance to bending strain than the H6R635 cable with Cu sheath. While H1R645 shows reduced current at around 70 mm, the H6R635 starts to degrade at higher diameter $-$120 mm. The presented characteristics of H6R635 shows $I_c(D)$ dependence similar to as observed for the monolithic MgB_2 tape with low strength Ni sheath. It has already been reported that the strength of individual components of the wire and more significantly, the outer sheath material, has a dominant effect on the bending strain tolerance of MgB_2 wires [14]; our results confirm this observation. The highest tolerance to bending strain has the MgB_2 cable with the MONEL® 400 sheath.

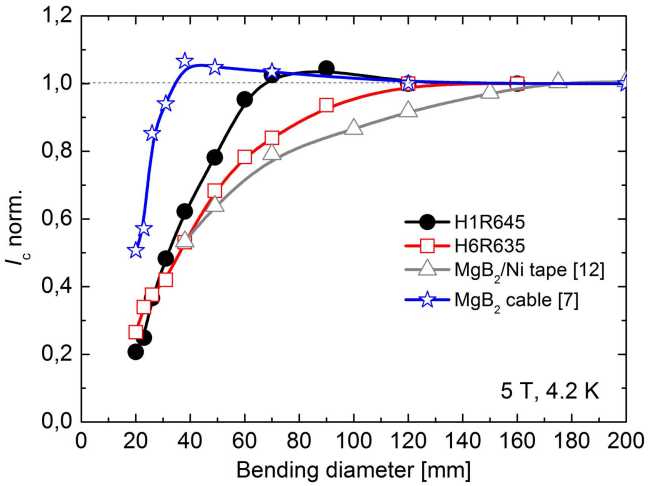

Figure 7. Critical current degradation of Rutherford MgB_2 cables by bending compared with behavior of monolithic 19 filaments MgB_2/Ni tape.

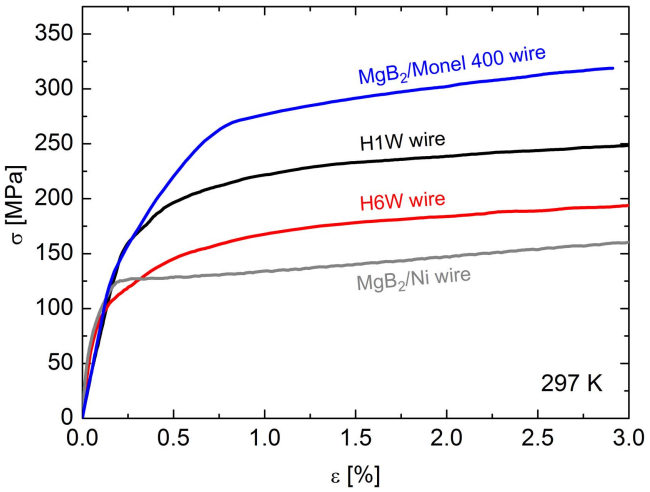

Figure 8. Stress−strain characteristics of strands H1W and H6W compared with monolithic 19 filaments MgB_2/Ni tape and single MgB_2/Monel wire.

In order to compare relation between $I_c(D)$ and stress −strain dependence we measured $\sigma(\varepsilon)$ characteristics of the individual wires at room temperature. Figure 8 shows a comparison of $\sigma(\varepsilon)$ characteristics of the single-core MgB_2 wire (with MONEL® 400 sheath) and monolithic MgB_2/Ni tape with the H1W and H6W strands. One can see that tolerances to bending strain plotted in figure 7 correspond to mechanical properties of these wires. Electro-mechanical measurements and testing of MgB_2 cables are also important for practical applications. They provide the data needed to understand the electrical performance of cables subjected to mechanical load. Therefore, stress−strain characteristics were measured for H1R and H6R cables in addition to the bending characteristics. Figure 9 shows $\sigma(\varepsilon)$ and $I_c(\varepsilon)$ characteristics of H1R628 and H6R635 samples measured in LHe at external magnetic field 6 T. Well visible are the elasto-plastic characteristics $\sigma(\varepsilon)$ of both samples which have beginning at very

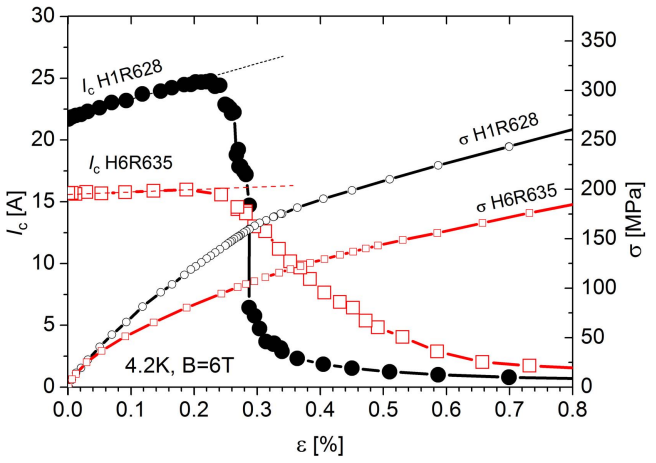

Figure 9. Stress−strain and $I_c(\varepsilon)$ characteristics of compacted H1R and H6R cables.

low strains. Strands in Rutherford cable are oriented along angular direction (angle of stranding) with respect to the cable longitudinal axis. Moreover strands are sharply bent on the cable edges where they have to make two bends in short succession. Unidirectional axial load applied to the flat cable induces complex of loads, e.g., stretching stiffness, tension, torsion and tension-induced bending of strands on the cable edges. As a result, the nonlinear elasto-plastic characteristics are expected for tension tests of flat cables which was found to be in reasonable agreement with the experimental data. $I_c(\varepsilon)$ characteristics plotted in figure 9 shows the apparent differences in I_c values and slope of the I_c increase with ε for both, the H1R628 and H6R635 samples. Monotonic flat $I_c(\varepsilon)$ characteristics up to ε_{irr} were measured for the high and low compacted H6R samples. It could be explained by the more plastic behavior of Cu sheath whereas, with H1R samples made of Cu10Ni sheath with higher strength, $I_c(\varepsilon)$ characteristics increase with the strain. Despite differences in mechanical properties of the outer sheaths of these two type of strands, similar irreversible strains of ε_{irr} ~0.24% were obtained for both types of cables. One explanation of obtaining the similar ε_{irr} limits was due to the solder plating applied to samples after the final heat treatment. The solder penetrated and filled voids in cable and partially soldered individual strands together. It caused improved transfer of the contact load between strands and predisposed to break the MgB_2 filaments at more uniform values. Tensile stress σ_{irr} corresponding to ε_{irr} was estimated to 140 MPa and 95 MPa for H1R and H6R cables, respectively.

In order to estimate performance of cables at cryogen-free applications, critical currents of individual strands H1W and H6W were measured also at elevated temperatures. Figure 10 shows $J_e(B)$ characteristics measured at temperature 15 K and 20 K. One can see that J_e values of the H6W wire are low and 10^4 A cm^{-2} cannot be reached at this temperature range (only in self-field at 4.2 K). More sharper $J_e(B)$ dependence is measured for H1W wire made of un-doped MgB_2 but $J_e = 10^4$ A cm^{-2} is reached at 2.6 T and 3.1 T, respectively. Therefore, this cable can be utilized for practical

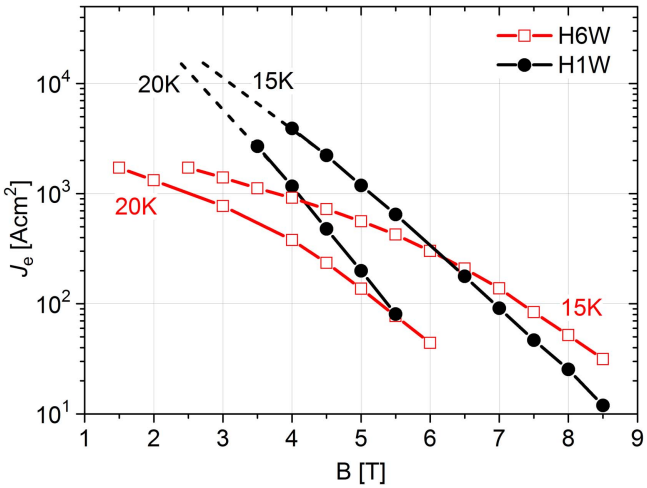

Figure 10. J_e(B) characteristics of H6W and H1W measured at temperature 15 and 20 K.

coils generating low fields at 4.2–20 K, e.g. for powerful wind turbines [15].

4. Conclusions

Two types of Rutherford MgB_2 cables with transposition length of 20 mm have been made from 12 *in situ* MgB_2 wires of outer diameter 390 μm manufactured by Hyper Tech Inc. The effect of cabling and compacting process to critical current of cables was evaluated. It was found that engineering current density of the Rutherford cable can be considerably increased by compaction (2.3−2.5 *x*), which is achieved by densification of Mg−B filaments prior to final heat treatment. Rutherford cable assembled of not-doped MgB_2 strands enables to reach the engineering current density 10^4 A cm^{-2} at external fields 2.6−4.0 T (20−4.2 K), which might be interesting for use in practical applications, e.g. for powerful wind turbine. Critical current degradation by bending begins at diameter below 70 mm for Cu10Ni sheathed strands, and 120 mm for Cu sheathed ones. The tolerance to bending strain is influenced dominantly by the mechanical strength of the outer sheath of strands.

Acknowledgments

This work was supported by the projects APVV-14-0522 and VEGA 2/0129/16

References

[1] Musenich R, Greco M, Razeti M and Tavilla G 2007 *Supercond. Sci. Technol.* **20** 235
[2] Kováč P, Hušek I and Melišek T 2008 *Supercond. Sci. Technol.* **21** 125003
[3] Holúbek T, Schlachter S I and Goldacker W 2009 *Supercond. Sci. Technol.* **22** 055011
[4] Kováč P, Hušek I, Rosová A, Melišek T and Kopera L 2010 *Supercond. Sci. Technol.* **23** 105006
[5] Schlachter S I, Braun U, Drechsler A, Goldacker W and Holúbek T 2010 *AIP Conf. Proc.* **1219** 302
[6] Hossain M S *et al* 2014 *Supercond. Sci. Technol.* **27** 095016
[7] Kopera L, Kováč P, Melišek T and Hušek I 2013 *Supercond. Sci. Technol.* **26** 125007
[8] Ballarino A 2010 *J. Phys.: Conf. Ser.* **234** 032003
[9] Kováč J, Šouc J, Kováč P, Hušek I and Gömöry F 2013 *Physica* C **495** 182
[10] http://hypertechresearch.com/
[11] Marzik J V, Lewis R C, Nickles M R, Finnemore D K, Yue J, Tomsic M, Rindfleisch M and Sumption M D 2010 *Proc. AIP Conf.* **1219** 295–302
[12] Kováč P, Kopera L, Melišek T, Sarmiento G, Sanz S, Brisigotti S, Nardelli D and Tropeano M 2015 *IEEE Trans. Appl. Supercond.* **25** 6200607
[13] MONEL® alloy 400 is trademark of Special Metals Corporation(www.specialmetals.com)
[14] Kováč P, Hušek I, Melišek T, Kulich M and Kopera L 2016 *Supercond. Sci. Technol.* **29** 045002
[15] Sanz S *et al* 2014 *J. Phys.: Conf. Ser.* **507** 032040